

DETC2006-99751

## THREE-DIMENSIONAL KINEMATIC ANALYSIS OF THE ACTUATED SPOKE WHEEL ROBOT

**Doug Laney**

Mechanical Engineering Department  
Virginia Polytechnic Institute and State University  
Blacksburg, Virginia 24061  
Email: dlaney@vt.edu

**Dennis Hong\***

Mechanical Engineering Department  
Virginia Polytechnic Institute and State University  
Blacksburg, Virginia 24061  
Email: dhong@vt.edu

### ABSTRACT

A current problem for mobile robots in unstructured environments is their lack of general mobility. Wheeled, treaded, and legged robots each have their advantages and disadvantages, but they all lack the flexibility to be able to cope with a wide range of terrain. The actuated spoke wheel system was presented in an earlier work as an alternative locomotive method that allows unique mobility capabilities to cope with various situations. This paper presents the three-dimensional kinematic analysis of the actuated spoke wheel system with no slip and no bounce constraints at the ground contacts for a robot using a two actuated spoke wheel configuration. The first analysis will cover the case when the axle is coplanar with the line connecting the contact points, called the pivot line, and show results from two examples, corresponding to steady state turning and, in the special case, straight-line walking. The second case will describe the configuration when the pivot line is skew with the axle, comparing the robot in this configuration to an SPPS spatial mechanism. This comparison will lead to the recommendation of a more general model, based on the SPPS mechanism, that will be used to analyze the motion in both configurations.

### 1 Introduction

At present, robots designed for unstructured environments tend to be specialized as their mobility is not yet robust enough to handle varying terrain [1]. Wheeled robots often have high efficiency and speed, but tend to be limited to relatively smooth

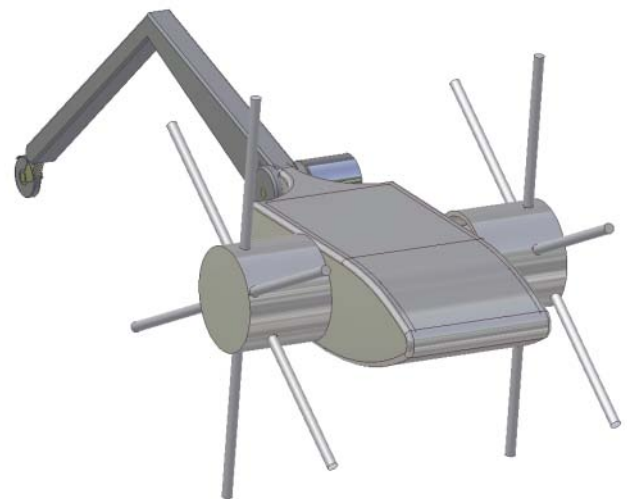


Figure 1. A proposed prototype that uses the two actuated spoke wheel configuration with a caster on an actuated tail

terrain. Legged robots are adaptable and have good mobility on rough terrain; however, the main disadvantage of legged mobile robots is that the complexity of the leg usually necessitates a slow and inefficient mechanism [2, 3].

The locomotive limitations of these two main types of mobile robots are currently countered in research by developing hybrid robots that add mechanisms to wheeled vehicles to give

\*Address all correspondence to this author.

them improved mobility, such as the expanding wheel vehicle which has four wheels that can expand based on polyhedral single degree-of-freedom expanding structures using prismatic joints [4] or the robot, Shrimp, developed by EPFL [5]. The Shrimp robot has six motorized wheels and uses a combination of actuation and passive mechanisms to raise and lower its wheels to climb objects up to twice the wheel diameter. Improvements to legged mobile robots look to improve the efficiency of the legged design, such as RHex, developed in part at the University of Michigan. RHex uses compliant legs in a hexapod configuration where each leg rotates full circle to walk a tripod gait [6, 7].

The research presented here is a step towards implementing the actuated spoke wheel system with an end goal to create a series of highly mobile robots known as the Intelligent Mobility Platform with Active Spoke System (IMPASS). IMPASS will use the actuated spoke wheel concept to cover various terrain with the unique ability to intelligently actuate its spokes to cope with obstacles at hand. Figure 1 shows one proposed prototype using two actuated spoke wheels with a caster on an actuated tail that would use the following analysis. Previous work has shown that the novel actuated spoke system has multiple modes of locomotion, presents some preliminary kinematic analysis, and outlines some potential uses for each mode [8].

This paper will establish two distinct classes of locomotion for the robot equipped with two actuated spoke wheels and create three-dimensional kinematic models with no-slip and no-bounce constraints to describe the motion for each class. One model will describe the motion for steady-state turning, i.e. motion with a constant turning radius. This model will also describe motion with an infinite turning radius, corresponding to straight steering. The second model will describe transient turning, which will be defined as turning at an increasing or decreasing rate. This will allow the robot to transition from navigating a straight line to a curved path and back again.

The distinguishing characteristic between these two classes of motion concerns the line connecting the foot-ground contact points, called the pivot line. Cases in which the pivot line is coplanar with the axle will create steady-state turning, while cases for which the pivot line is skew with the axle will create the transient turning. The special case for which the axle and pivot line are parallel create the straight steering case that creates a set of purely planar motions in the sagittal plane that are described in Reference [8]. After describing the models and illustrating some examples for the steady turning cases, this paper will describe future plans to create a general model based on the SPPS mechanism to analyze the motion in both configurations.

## 2 Kinematic Analysis

This section will define the geometry of the robot used to develop the models, then describe the kinematics for the case in which the pivot line is coplanar with the axle and show the joint

variables over the course of a step for two examples. Finally, the kinematics for the skew pivot line case will be described.

### 2.1 Defining the System Model

The model of the actuated spoke wheel for this paper is an extension of the model outlined in Reference [8]. The robot is considered to be constructed of two actuated spoke wheels set width  $w$  apart, with each wheel consisting of three actuated spokes of length  $L$  passing through the hub of the wheel, effectively acting as six actuated spokes per wheel. The coordinates for the model are as follows: the  $N$ -frame is a Newtonian frame attached to the smooth, flat terrain so that the  $\vec{n}_3$  vector is normal to the terrain. The  $P$ -frame is the path frame created by a rotation of angle  $\phi$  about the  $\vec{n}_3$  axis and is situated so that the robot is heading in the  $\vec{p}_1$  direction. The  $I$ -frame is an intermediate frame that is created by a rotation of angle  $\theta$  about the line connecting the contact points, defined by the  $\vec{p}_2$  vector. This frame defines the plane in which the robot rolls. The  $W$ -frame is the frame in which the wheels are fixed, and is created by a rotation of angle  $\psi$  about the  $\vec{l}_1$  axis, which accounts for roll of the body due to legs of unequal length. The body fixed frame,  $B$ , is fixed to the chassis of the robot and is defined by a rotation of  $-\theta$  about the  $\vec{w}_2$  axis.

Reference points on the geometry are used in the following derivations as shown in Figure 2. Note that the intermediate frame,  $I$ , is not used in the construction, and is therefore, not shown. The points  $A_R$  and  $A_L$  are the contact points and  $C_R$  and  $C_L$  are the hub centers of the right and left wheel respectively. The line passing through points  $A_R$  and  $A_L$  is the pivot line. Point  $G$  is the midpoint of the segment connecting  $C_R$  and  $C_L$ . Figure 1 shows the robot constructed with an actuated tail and caster wheel; however, for this analysis the tail will be idealized as a force that acts on the body along the  $\vec{n}_3$  direction (normal to the terrain), but will not affect the kinematics.

To fully define the position of the robot, the effective spoke length must be defined. Lengths  $r_{AR}$  and  $r_{AL}$  represent the distance from points  $A_R$  and  $A_L$  to  $C_R$  and  $C_L$ , respectively, and lie along the  $\vec{w}_3$  axis. The lengths  $r_{BR}$ ,  $r_{BL}$ ,  $r_{CR}$ , and  $r_{CL}$  represent the lengths from points  $C_R$  and  $C_L$  to the ends of the spokes that will next contact the ground during forward motion. Figure 3 shows these variables for one wheel.

### 2.2 Velocity Kinematics

The motion of the system will be derived by using the velocity kinematics. To completely define the position and orientation of the robot will require that some point on the robot be known as well as the configuration of the robot in that location. For the derivation here, the location of point  $G$  will be defined as  $x\vec{n}_1 + y\vec{n}_2 + z\vec{n}_3$  with  $\phi$ ,  $\theta$ ,  $\psi$ ,  $r_{AR}$ , and  $r_{AL}$  defining the pose. The state variable will then be  $x$ ,  $y$ ,  $z$ ,  $\phi$ ,  $\theta$ ,  $\psi$ ,  $r_{AR}$ , and  $r_{AL}$ . It is noted here that the motion of the spokes not in contact with the ground

is independent of the location and pose of the robot; therefore,  $r_{BR}$ ,  $r_{BL}$ ,  $r_{CR}$ , and  $r_{CL}$  are not listed as state variables. These state variables will be used to develop a set of kinematic differential equations (KDEs) which can then be numerically integrated to give the state variables as functions of time [9, 10].

The location of point  $G$  can be defined relative to the fixed point  $A_R$  located at  $(X, Y, Z)$  as

$$\begin{aligned} \vec{A_R G} &= r_{AR} \vec{w}_3 + \frac{w}{2} \vec{w}_2 \\ &= (x - X) \vec{n}_1 + (y - Y) \vec{n}_2 + (z - Z) \vec{n}_3. \end{aligned} \quad (1)$$

Therefore the velocity,  $V_{A_R}^G$ , of  $G$  relative to the fixed point  $A_R$  can be found as

$$\begin{aligned} \vec{V}_{A_R}^G &= \dot{r}_{AR} \vec{w}_3 + (\dot{\theta} \vec{p}_2 + \dot{\psi} \vec{i}_1 + \dot{\phi} \vec{n}_3) \times r_{AR} \vec{w}_3 \\ &\quad + (\dot{\psi} \vec{p}_1 + \dot{\phi} \vec{n}_3) \times \frac{w}{2} \vec{w}_2 \\ &= \dot{x} \vec{n}_1 + \dot{y} \vec{n}_2 + \dot{z} \vec{n}_3. \end{aligned} \quad (2)$$

Equation 2 can become quite cumbersome with all the involved coordinate transformations, but yields three scalar equations.

### 2.3 Kinematics For Coplanar Axle

At this point it becomes necessary to introduce the kinematic constraints that are specific to the case in which the pivot line is

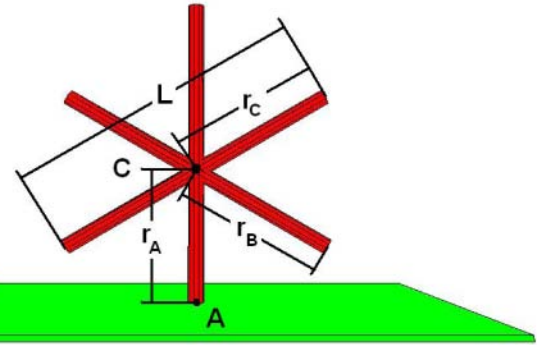


Figure 3. The lengths used to describe one wheel. A subscript R or L denotes right and left wheel, respectively

coplanar with the axle. For this analysis, it is assumed that only one spoke of each wheel remains in contact with the ground and does not slip or bounce. The wheels are also constrained to be in phase, which means that there is no difference in wheel angle,  $\theta$  for the two wheels. This constraint enforces that the pivot line is coplanar with the axle. The result of these constraints is that the left and right spokes in contact with the ground must change their length at the same rate in order to prevent skidding. This is stated mathematically as

$$\dot{r}_{AR} = \dot{r}_{AL}. \quad (3)$$

The no bounce constraint establishes that the roll angle  $\psi$  is purely a function of the effective spoke lengths. Therefore  $\psi$  can be defined as

$$\psi = \tan^{-1} \left( \frac{r_{AL} - r_{AR}}{w} \right). \quad (4)$$

Since it is a holonomic variable, it can be substituted into the other equations, and thereby reduce the rank of the KDEs by one, giving a total of seven independent state variables. The no slip constraint also implies that the heading angle cannot change during the course of a step. This implies that

$$\dot{\phi} = 0. \quad (5)$$

Reference [8] has shown that there are two degrees of freedom for the robot in this configuration: one that corresponds to pivoting about the line connecting the contact points  $A_R$  and  $A_L$  and another corresponding to the extension of the spokes in contact with the ground. Therefore, we are able to specify two additional arbitrary constraints. This analysis will consider only

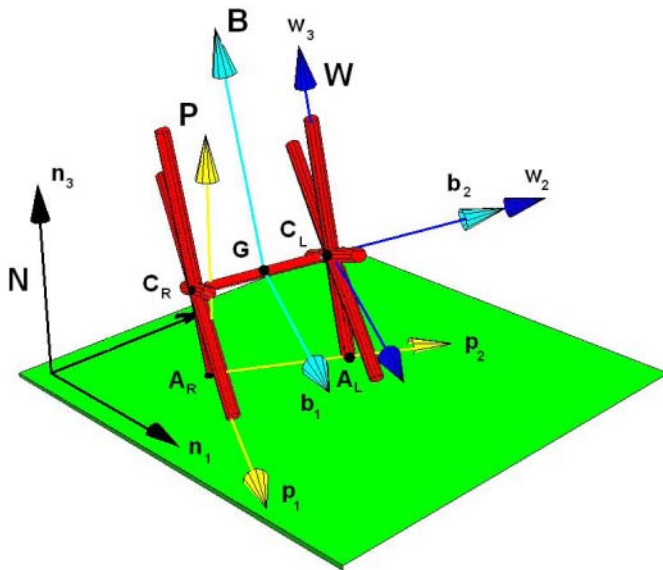


Figure 2. The frames and reference points used in construction of the model

those motions constrained such that the velocity along the heading  $\vec{p}_1$  is constant and the change in ride height of the body is zero. These constraints can be expressed mathematically as

$$\dot{x} = u_x \cos \phi \quad (6)$$

and

$$\dot{z} = u_z = 0. \quad (7)$$

The three equations from Equation 2 along with the four constraints given by Equations 3, 5, 6, and 7 result in a set of first-order, linear KDEs of the seven state variables and can be numerically integrated from a set physically possible initial conditions. This set of KDEs can be presented in the form

$$[C(t)] (\ddot{\vec{q}}) = (\vec{V}), \quad (8)$$

where  $C(t)$  is the matrix of time dependent coefficients of the state variables,  $\vec{q}$  are the state variables as listed above, and  $\vec{V}$  are the velocities. Taking the determinant of the matrix  $C(t)$  will show that

$$|C(t)| = \frac{w(r_{AR} + r_{AL})(w \cos \phi + \sin \theta \sin \phi (r_{AL} - r_{AR}))}{2(w^2 + (r_{AL} - r_{AR})^2)}, \quad (9)$$

which means except for the cases when  $r_{AR} + r_{AL} = 0, w = 0$ , or  $r_{AR} = r_{AL}$  with  $\phi = n\pi/2$  for odd  $n$ , the matrix is invertible. So for cases in which the robot does not rest with its axle on the ground, or with no width,  $w$ , and since  $\dot{\phi} = 0$  the solution will not move through a non-invertible position over the course of the integrated step. This system may be used to calculate the position of the robot when it does not start in a non-invertible position.

## 2.4 Motion Profiles

Using the results of the above kinematic analysis, it is now possible to consider certain motions and integrate to observe the resulting state variables over the course of a single step. Reference [8] has shown that the actuated spoke wheel setup has a periodic gait for both straight-line walking and steady turning. Both of these cases are considered below, and the resulting state variables are plotted and discussed.

**2.4.1 Straight-line walking** For the case of straight line walking, the initial conditions are specified such that

$r_{AR}(0) = r_{ARo}, r_{AL}(0) = r_{ALo}, \phi(0) = \phi_o, \theta(0) = \theta_o$  with the additional consideration that point  $A_R$  is initially located at  $(X, Y, Z)$  in the  $n$ -frame, then the starting location of point  $G$  can be found by using equation 1.

The geometric constants  $w$  and  $L$  are chosen based on the proposed prototype shown in Figure 1 such that  $w = 0.3\text{m}$  and  $L = 0.6\text{m}$ . For steady walking over flat terrain, a step occurs over a range of  $-\pi/6 \leq \theta \leq \pi/6$ , therefore  $\theta_o = -\pi/6$ . The leg lengths are chosen to be initially  $r_{ARo} = r_{ALo} = 0.3\text{m}$  since the legs must be of equal length for straight-line motion.  $\phi_o = 0$  is chosen for the heading angle, and the reference point  $A_R$  is chosen to be at  $(0,0,0)$  in the  $N$ -frame. Furthermore, it is considered that the robot is moving such that its speed is a constant speed of  $0.3\text{m/s}$  along its heading angle and that the body of the robot remains parallel to the flat terrain. Referring to Equations 6 and 7, this corresponds to  $u_x = 0.3\text{m/s}$  and  $u_z = 0\text{m/s}$ . At this point Mathematica is used to integrate the KDEs over a single step, which for the chosen constants is one second. The results are plotted in Figure 4.

It can be seen from Figure 4 that the motion is as expected for the simple case. The effective spoke lengths for each side are equal for the entire duration of the step. Each starts at the initial length, decreases to a minimum when the axle is directly above the pivot line (at the midpoint of the step), then increases again to the starting value. The heading angle,  $\phi$ , does not change during the course of the step. The wheel angle,  $\theta$ , increases smoothly, though not linearly for the entire step, varying from  $-\pi/6$  to  $\pi/6$ . The coordinates of point  $G$  increases linearly in  $x$  and remains constant in  $y$  and  $z$ . The body roll angle,  $\psi$ , is not plotted since it is a direct function of the effective spoke lengths. At the conclusion of this step, the state information could be passed again to the numeric integrator, and the process could be repeated for the subsequent step.

**2.4.2 Steady state turning** Steady state turning is considered for this analysis to be turning at a constant rate without changing from one effective turning radius to another. As established in Reference [8], turning for the robot equipped with actuated spoke wheels is performed discretely. Since the no slip constraints prohibit any change in heading angle during a step, what must occur is a change in the heading angle,  $\phi$ , from one step to the next. The robot can be considered to be pivoting about the pivot line (the line connecting the two contact points); therefore, turning occurs discretely when the pivot line for a step is not parallel to the pivot line for the previous step. If the robot starts in a configuration with the same effective spoke length for each wheel, it will move directly along the heading angle as illustrated in the previous example. If the robot continues to select the same effective spoke length for each subsequent step, the pivot lines for each step will be parallel, and the robot will continue in a straight path.

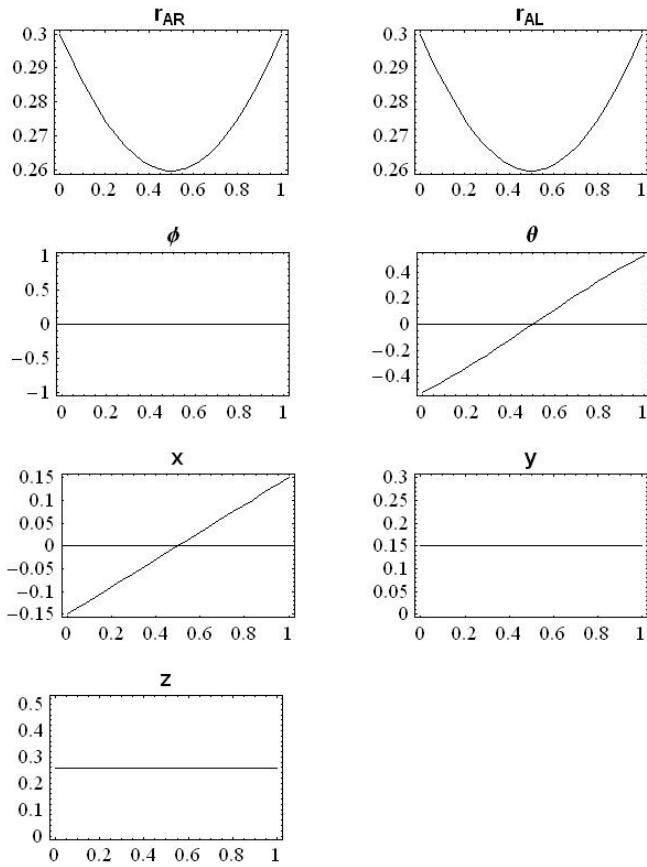


Figure 4. Results from numeric integration of KDEs for straightline walking. Plots show state variables versus time for a single step

However, if the robot begins in a configuration in which the effective spoke lengths are different, and it continues to use the same effective spoke lengths from step to step, then one side of the robot will take a "longer step" than the other. This will cause the pivot line not to be parallel for each subsequent step, creating a discrete amount of turning from step to step. It is possible to use the same KDEs to determine the state variables during the course of a turning step, since the motion for each step occurs directly along the heading angle.

To analyze a case of steady state turning, one can use the above initial conditions, but let  $r_{ALo} = 0.3\text{m}$  and let  $r_{ARo} = 0.25\text{m}$ . For that case, the results are shown in Figure 5. One can see from the plots that the leg positions move together, they are simply offset by a constant value from the initial conditions. The turning can be verified by the change in angle of the new pivot line for the next step, defined by the two new contact points. The other variables again progress through their expected values. The one key distinction is that in the turning case, there is some motion in the lateral direction from the change in lengths of the

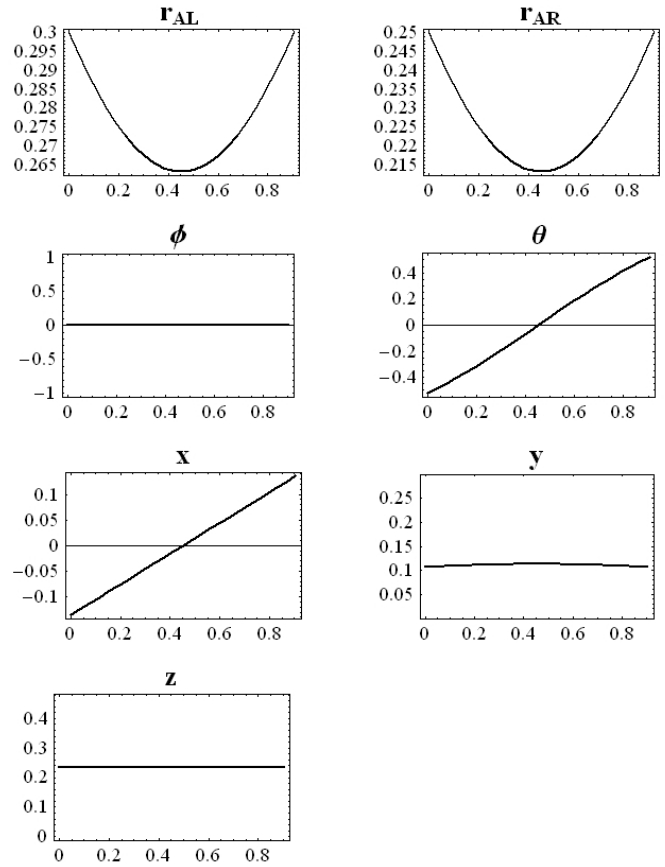


Figure 5. Results from numeric integration of KDEs for steady state turning. Plots show state variables versus time for a single step. Note the slight motion induced in the Y-direction from actuating the spokes while the spokes are not vertical

spokes while the robot is not vertical.

## 2.5 Kinematics for Skew Axle

The motion of the robot with the axle skew to the pivot line will occur at the end of a step as described above. In a step as described above, there will be two points in contact with the ground, and the pivot line connecting these points is always coplanar with the axle. At the end of the step, the next pair of spokes will have the same lengths respectively as those in current contact with the ground and will contact at the same time, giving four contact points at the transition. The pivot line for the subsequent step, created by the next pair of spokes making contact, will be coplanar with the axle again and will give steady turning or straight steering.

Creating transient turning without introducing bouncing or slipping at the contacts can be accomplished by having the spoke

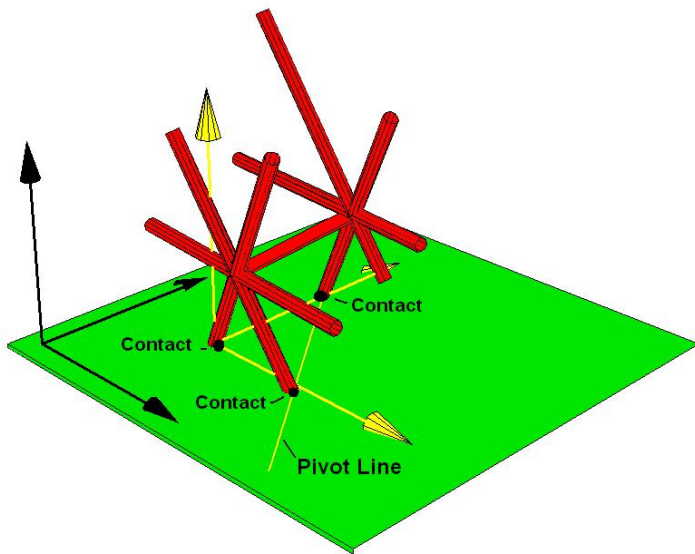


Figure 6. Transient turning is created by intelligently actuating the spokes such that there are three contact points at the transition, creating a pivot line that is skew to the axle. An obvious degree of freedom in this configuration is available by rotating about the pivot line

lengths chosen for the subsequent step to be different from the spoke lengths of the current contact points, such that at the transition, there will be only three points of contact. Therefore, the first phase of a transient turning step would be described by the model above; however, the second phase would be fundamentally different. The contact points would be on spokes that are separated by  $60^\circ$  instead of spokes that are parallel. This would cause the pivot line to be skew with the axle. Figure 6 shows this idea.

In this configuration, there is an obvious degree of freedom in that the robot can pivot about the line connecting the contact points. It is worth noting that if the third contact point at the transition is on the right actuated spoke wheel, the robot will tip to the left, creating a left turning motion. Likewise, the third contact at transition on the left actuated spoke wheel will create a right turning motion. This is an interesting result because it gives the motion planner the option to create a right turn either by shortening the right spoke, extending the left spoke, or some combination of the two, and likewise for creating a left turn.

Additional insight of this configuration came from performing a mobility analysis on the robot in this configuration. Kinetically, it can be represented as an SPPS spatial mechanism, which has two degrees of freedom. By fixing the rotation about the pivot line and studying the remaining motion, it was noticed that there is a motion possible in the parallel planes containing the actuated spoke wheels, and this motion corresponds exactly to the two-point contact scheme described in Reference [8]. Figure 7 shows the spatial configuration of the robot projected onto

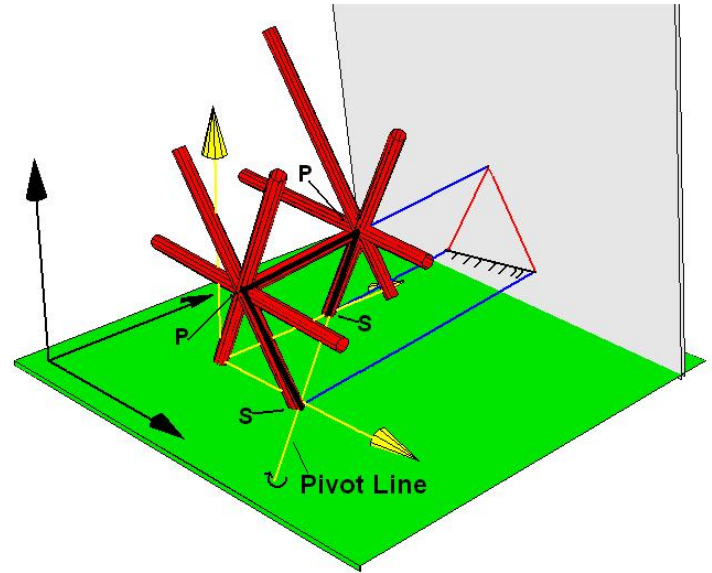


Figure 7. The second degree of freedom is a planar motion. The mechanism is projected onto the plan containing the actuated spoke wheels to emphasize the available motion

the wheel frame. Figure 8 shows the type of motion that would be permissible in the projected plane.

With the two degrees of freedom in this configuration firmly established, creating a set of kinematic differential equations in terms of the seven state variables could be accomplished in a similar fashion as described above. The transient turning could be considered the second phase of a step in which the first phase is described in the coplanar kinematics section. The motion in the transient turning would be defined by the planar motion as illustrated in Figure 8 as that plane is rotated about the pivot line as shown in Figure 7.

With the insight gained from considering the robot in this configuration to be an SPPS mechanism, the authors are focusing on creating a more general kinematic model based on the spatial mechanism. This model would have a parameter that defines the angle between the spokes in contact with the ground. This approach will allow us to describe the case of transient turning

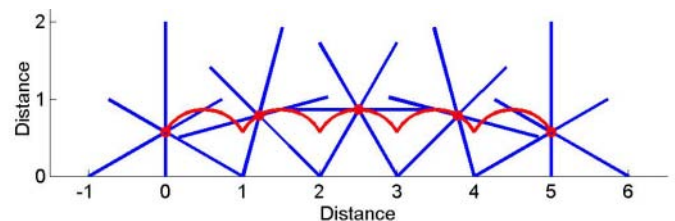


Figure 8. An example of the type of motion available within the wheel plane

in which there is a large angle between the spokes that are in contact with the ground, creating a skew pivot line, as well as to describe the case where there is a zero angle between the spokes in contact, creating the coplanar pivot line, which generates the steady turning motions. This model would have the added benefit of being able to describe motions in which the actuated spoke wheels are differentially driven, i.e. the angle between the spokes in contact with the ground is between  $0^\circ$  and  $60^\circ$ . The results from this more general model would allow for kinematic analysis of the robot in a variety of configurations and actuation strategies including differential steering.

### 3 Conclusion

In this paper, a model for a kinematic analysis of the position as a function of time of the robot equipped with two actuated spoke wheels is presented for the case in which the line connecting the contact points, or pivot line, is coplanar with the axle of the robot. The robot is defined by seven independent state variables. Using no slip and no bounce constraints at the contact point with two arbitrary inputs, a set of kinematic differential equations is developed. These are numerically integrated yielding position information as a function of time. This numeric integration is used to report the joint variables over the course of a single step for both a steady state turning step, and a straight steering step.

The concept for transient turning is then introduced by having three contact points at the step transition, forcing the pivot line to be skew with the axle of the robot. Insight into this configuration was gained by analyzing the robot in this configuration as an SPPS spatial mechanism. The motion created by this configuration is then described qualitatively. The insight gained from the spatial analysis is used to describe a more general kinematic model that could be used to analyze both cases of the coplanar pivot line and the skew pivot line, as well as allow analysis of the effects of differentially driving the two actuated spoke wheels.

### 4 Future Work

The kinematic cases presented for the coplanar pivot line are simple ones, with constant velocity along the heading angle,  $\phi$ , and zero velocity normal to the terrain; however, the velocities are arbitrary, and need not be constant. The KDEs presented here can be used to solve for the state variables when presented with sinusoidal motion, or any other type of functional input. One of the promising future research interests is to study the inverse of the problem presented here: not making arbitrary motion over smooth terrain, but instead studying the application of generating smooth motion over varying terrain.

Additionally, only a preliminary discussion of the more general kinematic model that would describe the transient turning,

steady state turning, and differential drive of the actuated spoke wheels is covered here. A complete mathematical analysis of the more general model is currently underway and will be presented in a future publication.

### Acknowledgment

We would like to thank Virginia Tech for partially funding this research through the ASPIRES award and the National Science Foundation for their continued support of this work.

### REFERENCES

- [1] Hong, D. W., and Cipra, R. J., 2006. "Visualization of the contact force solution space for multi-limbed robots". *ASME Journal of Mechanical Design*, **128**(1), pp. 295–302.
- [2] Siegwart, R., and Nourbakhsh, I. R., 2004. *Introduction to Mobile Robots*. The MIT Press, Cambridge, MA.
- [3] Todd, D., 1985. *Walking Machines: An Introduction to Legged Robotics*. Kogan-Page, London.
- [4] Agrawal, S. K., and Yan, J., 2003. "A three-wheel vehicle with expanding wheels: Differential flatness trajectory planning and control". In Proceedings of the 2003 IEEE/RSJ International Conference on Intelligent Robots and Systems.
- [5] Siegwart, R., Lamon, P., Estier, T., Lauria, M., and Piguet, R., 2002. "Innovative design for wheeled locomotion in rough terrain". *Journal of Robotics and Autonomous Systems*, **40**(4), pp. 151–162.
- [6] Saranli, U., Buehler, M., and Koditschek, D. E., 2001. "Rhex: A simple and highly mobile hexapod robot". *The International Journal of Robotics Research*, **20**(7), pp. 616–631.
- [7] Saranli, U., Buehler, M., and Koditschek, D. E., 2001. "Design, modeling and preliminary control of a compliant hexapod robot". In Proc. IEEE International Conference on Robotics & Automation.
- [8] Laney, D., and Hong, D., 2005. "Kinematic analysis of a novel rimless wheel with independently actuated spokes". In Proceedings of the 29th ASME Mechanisms and Robotics Conference.
- [9] Dankowicz, H., 2005. *Multibody Mechanics and Visualization*. Springer-Verlag, New York.
- [10] Hahn, H., 2002. *Rigid Body Dynamics of Mechanism, Vol 1: Theoretical Basis*. Springer-Verlag, New York.